Testability of the model by the collider and gravitational wave experiments

Katsuya Hashino (Center for High Energy Physics, Peking University)

Collaborators: R. Jinno [1, 2], M. Kakizaki [3], S Kanemura [4], T. Takahashi [5], M Takimoto [2, 6]

(1. IBS, 2. KEK, 3. Univ. of Toyama, 4. Osaka Univ., 5. Saga Univ., 6. Weizmann Institute of Science)

[K. H, R. Jinno, M. Kakizaki, S. Kanemura, T. Takahashi and M. Takimoto, Phys. Rev. D 99, no. 7, 075011 (2019)]

Introduction

- Higgs boson which is predicted in the Standard Model (SM) was detected at the Large Hadron Collider(LHC).

- Measurements of Higgs boson couplings

Image of SM

The relation between the mass of particle and Higgs coupling in the SM

$$m_i \sim y_i v$$
$$m_j \sim g_j^{1/2} v$$

m_i : Mass of particle i (quark and lepton)

m_j : Mass of gauge boson j

y_i : Yukawa interaction for fermion i

g_j : Higgs couplings for gauge boson j

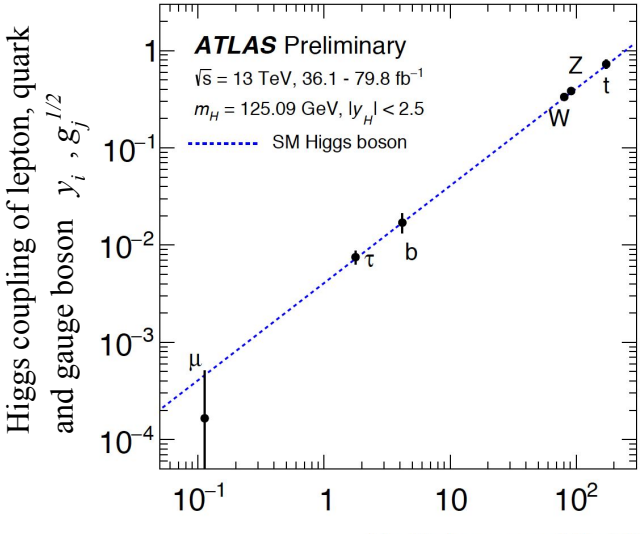

[The ATLAS collaboration [ATLAS Collaboration], ATLAS-CONF-2018-031]

The SM can explain the current results of the collider experiments below O(1) TeV.

Introduction

❖ However, phenomena beyond the SM have been reported.

- Dark matter
- Neutrino oscillations
- Baryon asymmetry of the Universe (BAU)

→ The SM has to be extended.

❖ The Higgs sector is still vague.

- The number of the Higgs field ?
- The Higgs field is elementary or composed ?
- Dynamics of the electroweak symmetry breaking (EWSB) ?

→ Various extended Higgs models

❖ The extended Higgs models can explain phenomena beond the SM.

Figure 1 : SM is not a perfect SuperMan (SM)...

Figure 2 : New physics model beyond SM as an example

Introduction

❖ Electroweak Baryogenesis (EWBG) is a senario explaining BAU.

Sakharov's conditions

[A. D. Sakharov, Pisma Zh. Eksp. Teor. Fiz. 5, 32 (1967)]

- Baryon number violation
  → Sphaleron process
- C and CP violation
  → Extended Higgs sector
- Departure from equilibrium
  → Strongly first order electroweak phase transition (1st EWPT) ($\varphi_c / T_c \gtrsim 1$)

The SM cannot satisfy the condition of strongly 1st EWPT $\varphi_c / T_c \gtrsim 1$.

[Y. Aoki, F. Csikor, Z. Fodor and A. Ukawa, Phys. Rev. D 60, 013001 (1999)]

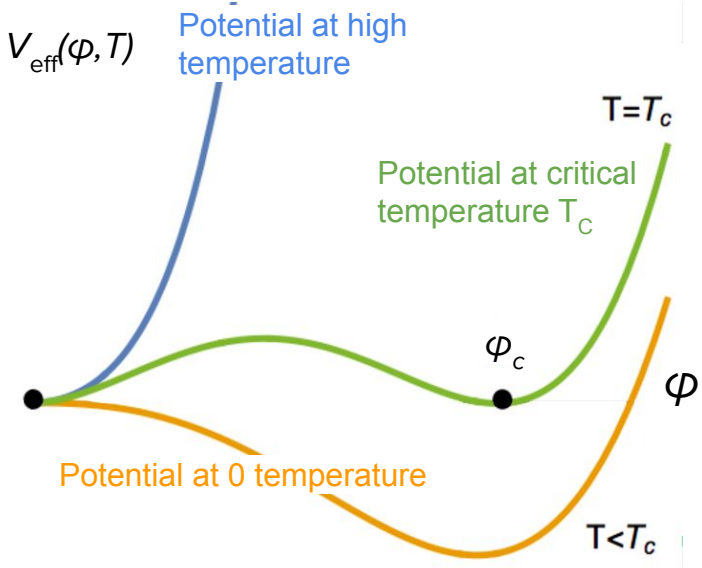

❖ We can realize strongly 1st EWPT by extended Higgs models.

How do we test the models with strongly φ_c / T_c ?

Test of the model with strongly 1st EWPT

- The model can realize $\varphi_c / T_c \gtrsim 1$ when *hhh* coupling is about 10% larger than the SM one.

[S. Kanemura, Y. Okada and E. Senaha, Phys. Lett. B 606, 361 (2005)]

⇒ We can use measurements of Higgs boson coupling by **collider experiments** to test the model with $\varphi_c / T_c \gtrsim 1$.

- The gravitational waves (GWs) occur when the model realizes the 1st EWPT.

GWs are produced by collision of true vacuum bubbles.

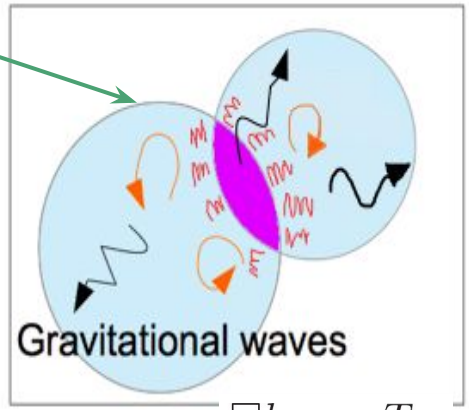

$\Box h_{\mu\nu} \sim T_{\mu\nu}$

The spectrum of the GW is characterized by the following parameters:

α ≃ Normalized latent heat released by EWPT, β ≃ 1/(Duration of EWPT)

T_t ≃ Temperature at the end of EWPT, v_b ≃ Velocity of bubble wall

These values have the information about Higgs potential

[A. Kosowsky, M. S. Turner, and R. Watkins, Phys. Rev. D45 (1992) 4514, Phys. Rev. Lett. 69 (1992) 2026]

⇒ We can use **GW observation experiment** to test the model with $\varphi_c / T_c \gtrsim 1$.

In this talk

- We can discuss expected uncertainties in GW observation experiments for parameters of the extended models by the fisher matrix analysis.

  (The fisher matrix corresponds to the inverse of the covariance matrix.)

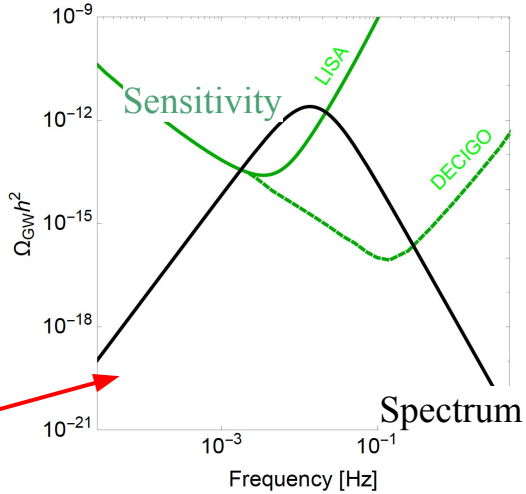

In this case, we can get parameter informations by the GW measurement.

- We quantitatively discuss a testability of a real Higgs singlet model by the synergy between the collider and GW observation experiment.

[K. H. , R. Jinno, M. Kakizaki, S. Kanemura, T. Takahashi and M. Takimoto, Phys. Rev. D 99, no. 7, 075011 (2019)

Real Higgs singlet model

Motivation

❖ Model with strongly 1st EWPT

$$V_{\text{eff}}(\varphi, T) = D(T - T_0)\varphi^2 + (e - ET)\varphi^3 + \frac{\lambda(T)}{4}\varphi^4$$

e : tree-level effects

E : thermal loop effect of bosons

(Potential with high temperature approximation)

$$\frac{\varphi_C}{T_C} = \frac{2}{\lambda(T_C)}\left(E - \frac{e}{T_C}\right)$$

- The model in which the mixing effects e at tree-level is mainly related to 1st EWPT
- The model in which the loop effects of bosons E is mainly related to 1st EWPT

Real Higgs singlet model is one of the simplest model with small e effects.

Motivation

- Model with strongly 1st EWPT

$$V_{\text{eff}}(\varphi, T) = D(T - T_0)\varphi^2 + (e - ET)\varphi^3 + \frac{\lambda(T)}{4}\varphi^4$$

e : tree-level effects

E : thermal loop effect of bosons

(Potential with high temperature approximation)

$$\frac{\varphi_C}{T_C} = \frac{2}{\lambda(T_C)}\left(E - \frac{e}{T_C}\right)$$

Higgs boson couplings for fermion and gauge boson can affect the value of φ_C/T_C .

lated to 1st EWPT

ed to 1st EWPT

Real Higgs singlet model is one of the simplest model with small e effects.

Model with a real isospin singlet scalar field

[K. H. , M. Kakizaki, S. Kanemura, P. Ko and T. Matsui, Phys. Lett. B766 (2017) 49]

- This model is the SM with one isospin singlet scalar field S.

- Higgs potential

$$V_0 = \underbrace{-\mu_\Phi^2|\Phi|^2 + \lambda_\Phi|\Phi|^4}_{\text{The SM parts}} + \underbrace{\mu_{\Phi S}|\Phi|^2 S + \frac{\lambda_{\Phi S}}{2}|\Phi|^2 S^2 + \mu_S^3 S + \frac{m_S^2}{2}S^2 + \frac{\mu'_S}{3}S^3 + \frac{\lambda_S}{4}S^4}_{\text{An additional scalar boson parts}}$$

$$\Phi = \begin{pmatrix} \phi^+ \\ \frac{1}{\sqrt{2}}(\phi_1 + i\phi_0) \end{pmatrix} \qquad S = \phi_2 \qquad \langle\Phi\rangle = \begin{pmatrix} 0 \\ \frac{1}{\sqrt{2}}v \end{pmatrix} \quad \langle S\rangle = v_S$$

  - Stationary condition of the potential

$$\left.\frac{\partial V}{\partial \phi_i}\right|_{\phi_1=v,\phi_2=v_S} = 0, \ (i = 1, 2)$$

Model with a real isospin singlet scalar field

[K. H. , M. Kakizaki, S. Kanemura, P. Ko and T. Matsui, Phys. Lett. B766 (2017) 49]

- Diagonalized mass matrix for SM-like Higgs *h* and additional scalar *H*

$$\begin{pmatrix} h \\ H \end{pmatrix} = \begin{pmatrix} \cos\theta & -\sin\theta \\ \sin\theta & \cos\theta \end{pmatrix} \begin{pmatrix} \phi_1 \\ \phi_2 \end{pmatrix}$$

$$\begin{pmatrix} m_h^2 & 0 \\ 0 & m_H^2 \end{pmatrix} = \begin{pmatrix} \cos\theta & \sin\theta \\ -\sin\theta & \cos\theta \end{pmatrix} \begin{pmatrix} m_{11}^2 & m_{12}^2 \\ m_{21}^2 & m_{22}^2 \end{pmatrix} \begin{pmatrix} \cos\theta & -\sin\theta \\ \sin\theta & \cos\theta \end{pmatrix}$$

Mass matrix for *h* and *H*

Mass matrix for ϕ_1 and ϕ_2 $\quad m_{ij}^2 = \left. \dfrac{\partial^2 V_{\mathrm{eff},T=0}}{\partial\varphi_i \partial\varphi_j} \right|_{\phi_1=v,\phi_2=v_S}$

- Independent parameters of the model

μ_Φ, λ_Φ, $\mu_{\Phi S}$, $\lambda_{\Phi S}$, μ_S, m_S, μ'_S, λ_S → $v\ (246GeV), m_h(125GeV), v_S, m_H, \theta, \mu_S, \mu'_S, \mu_{\Phi S}$

(Parameters in tree-level potential)

Model with a real isospin singlet scalar field

[K. H. , M. Kakizaki, S. Kanemura, P. Ko and T. Matsui, Phys. Lett. B766 (2017) 49]

- Scaling factors of the Higgs boson coupling

$$\kappa_X \equiv \frac{g_{hXX}}{g_{hXX}^{\rm SM}}, \quad \kappa = \kappa_V = \kappa_F = \cos\theta$$

g_{hXX} : Higgs coupling for X,
V : gauge boson,
F : fermion

(It is the ratio between the coupling of the real Higgs singlet model and one of the SM.)

- The deviation for *hhh* coupling

$$\frac{\Delta\lambda_{hhh}}{\lambda_{hhh}^{SM}} = \frac{\lambda_{hhh}-\lambda_{hhh}^{SM}}{\lambda_{hhh}^{SM}} \qquad \lambda_{hhh} = c_\theta^3 \left\langle \frac{\partial^3 V_{\rm eff,T=0}}{\partial\varphi_\Phi^3} \right\rangle + c_\theta^2 s_\theta \left\langle \frac{\partial^3 V_{\rm eff,T=0}}{\partial\varphi_\Phi^2 \partial\varphi_S} \right\rangle + c_\theta s_\theta^2 \left\langle \frac{\partial^3 V_{\rm eff,T=0}}{\partial\varphi_\Phi \partial\varphi_S^2} \right\rangle + s_\theta^3 \left\langle \frac{\partial^3 V_{\rm eff,T=0}}{\partial\varphi_S^3} \right\rangle$$

These Higgs couplings can be precisely measured by future collider experiments.

Results

Model with a real isospin singlet scalar field

- The benchmark point and scanned range

v_Φ [GeV]	v_S [GeV]	m_h [GeV]	$\mu_{\Phi S}$ [GeV]	μ'_S [GeV]	μ_S [GeV]	m_H [GeV]	θ [degrees]
246.2	90	125.5	−80	−30	0	[160, 240]	[−45, 0]

[K. Fuyuto and E. Senaha, Phys. Rev. D 90, 015015 (2014)]

(We analyze the EWPT in multi-field space by public code "CosmoTransitions".)

[C. L. Wainwright, Comput. Phys. Commun. 183, 2006 (2012)]

$$\Delta\lambda_{hhh} = \frac{\lambda_{hhh}^{\rm HSM} - \lambda_{hhh}^{\rm SM}}{\lambda_{hhh}^{\rm SM}}, \qquad \kappa_X \equiv \frac{g_{hXX}}{g_{hXX}^{\rm SM}}, \qquad \kappa = \kappa_V = \kappa_F = \cos\theta$$

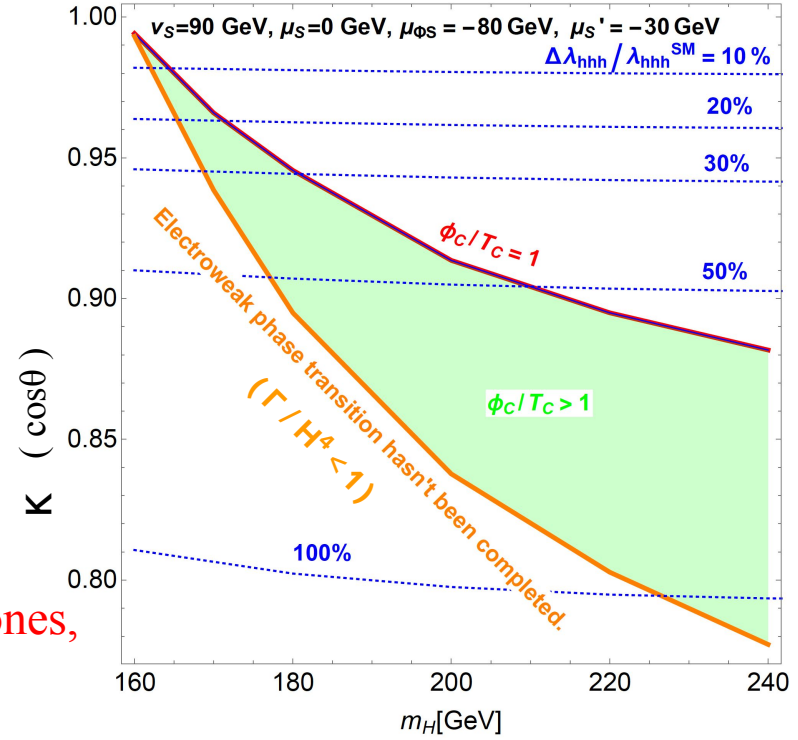

(Mass of new particle)

- The Higgs boson couplings deviate from the SM ones, when the model can realize strongly 1st EWPT.

Also detectable GWs from the EWPT may be able to occur.

Model with a real isospin singlet scalar field

- We show the parameter region where the detectable GW spectrum occurs.

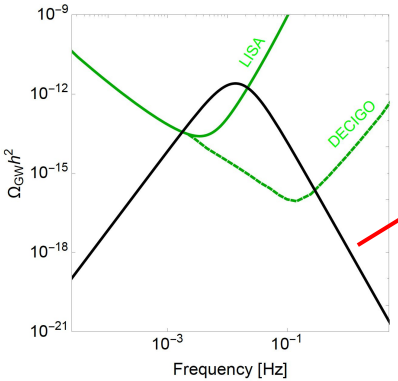

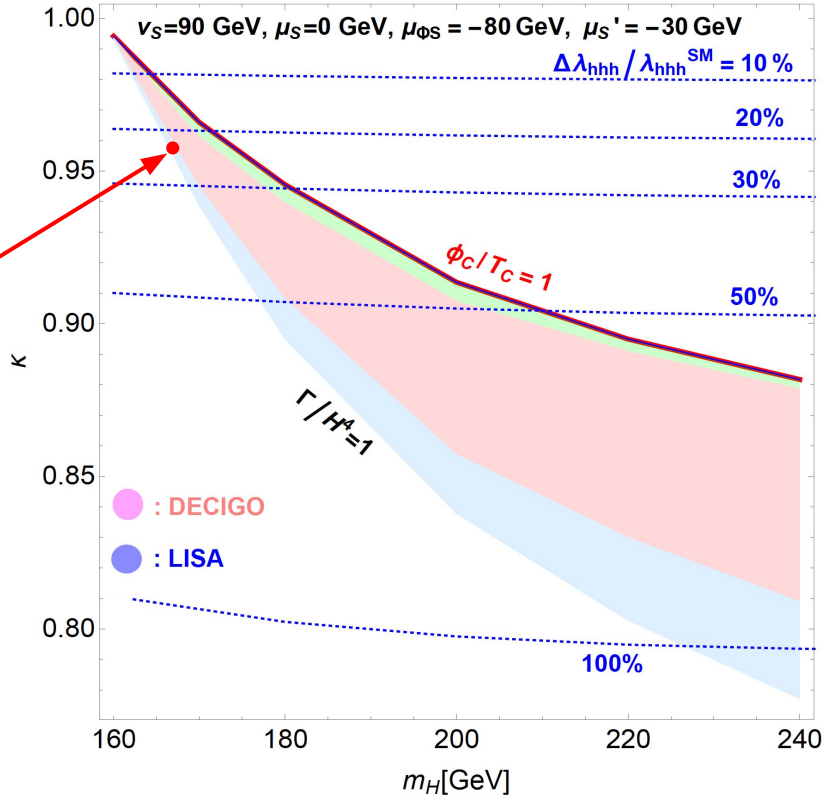

- We conclude that the model with strongly 1st EWPT can be complementarily tested by the measurements of hff and hVV couplings at LHC, ones of hhh coupling at ILC and ones of the spectrum of the GW at DECIGO and LISA.

[K. H. , M. Kakizaki, S. Kanemura, P. Ko and T. Matsui, Phys. Lett. B766 (2017) 49]

Testability of real Higgs singlet model

- Fiducial point (m_H, κ) = (166.4 GeV, 0.96)

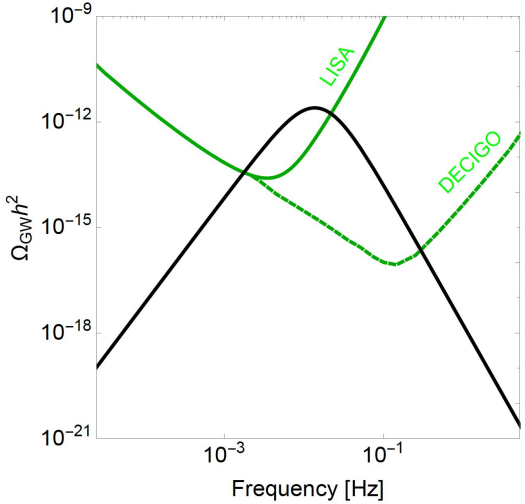

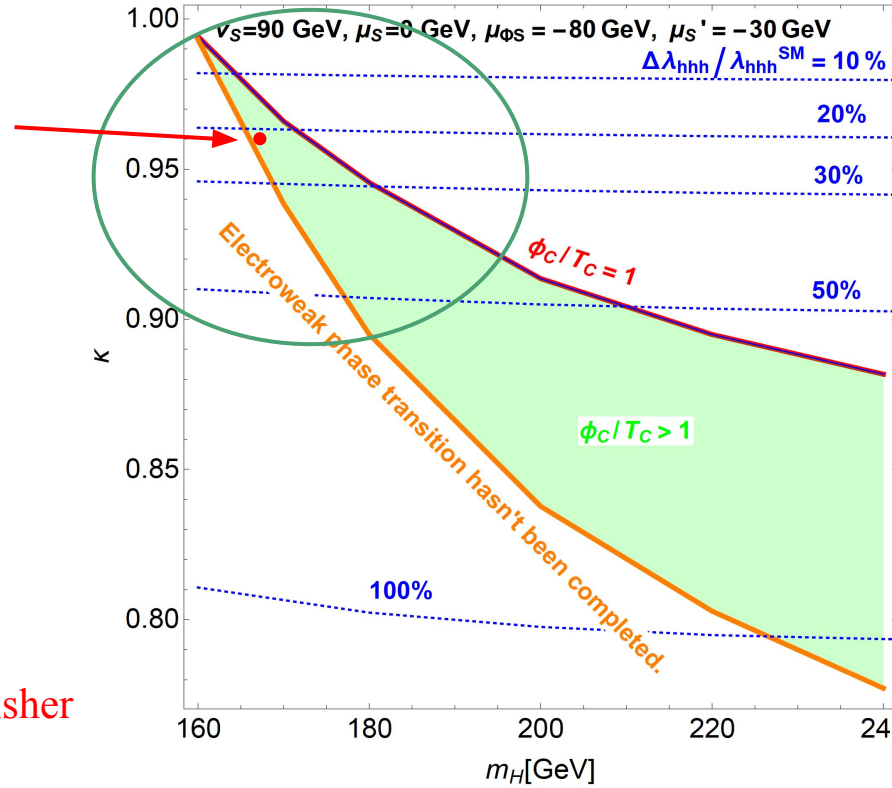

- We can estimate the expected constraints by the Fisher matrix analysis, which is essentially a Gaussian approximation of the likelihood function.

Testability of real Higgs singlet model

- $\Delta\lambda_{hhh}/\lambda_{hhh}^{SM}$ and detectable GWs are described in scaling factors (κ_F and κ_V) and m_H.

$$\frac{\Delta\lambda_{hhh}}{\lambda_{hhh}^{SM}} = \frac{\lambda_{hhh}-\lambda_{hhh}^{SM}}{\lambda_{hhh}^{SM}}, \quad \kappa_X \equiv \frac{g_{hXX}}{g_{hXX}^{\rm SM}}, \quad \kappa = \kappa_V = \kappa_F = \cos\theta$$

- Fiducial point (m_H, κ) = (166.4 GeV, 0.96)

  ILC : $\Delta\kappa_Z \sim 0.38\%$ [K. Fujii et al., arXiv:1710.07621 [hep-ex]]

  Direct searches by LHC Run-II :

  [A. Ilnicka, T. Robens, and T. Stefaniak, Mod. Phys. Lett. A33 no. 10n11, (2018) 1830007]

- We may be able to test the model by the synergy between measurements of the Higgs boson couplings and the spectrum of GW.

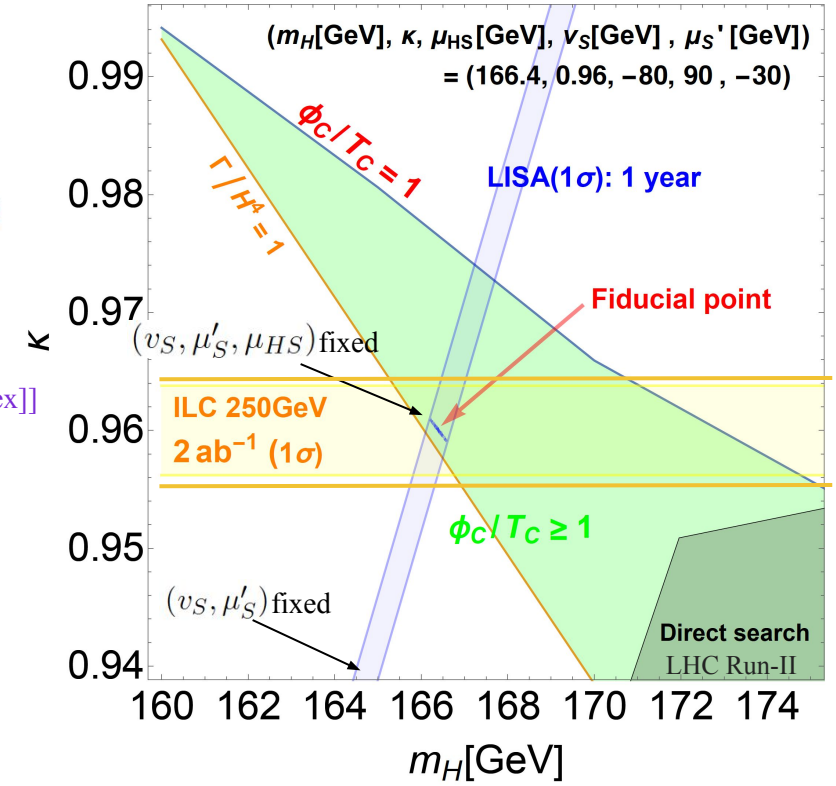

[K. H, R. Jinno, M. Kakizaki, S. Kanemura, T. Takahashi and M. Takimoto, Phys. Rev. D 99, no. 7, 075011 (2019)]

Testability of real Higgs singlet model

- $\Delta\lambda_{hhh}/\lambda_{hhh}^{SM}$ and detectable GWs are described in scaling factors (κ_F and κ_V) and m_H.

$$\frac{\Delta\lambda_{hhh}}{\lambda_{hhh}^{SM}} = \frac{\lambda_{hhh}-\lambda_{hhh}^{SM}}{\lambda_{hhh}^{SM}}, \quad \kappa_X \equiv \frac{g_{hXX}}{g_{hXX}^{\rm SM}}, \quad \kappa = \kappa_V = \kappa_F = \cos\theta$$

- Fiducial point (m_H, κ) = (166.4 GeV, 0.96)

  ILC : $\Delta\kappa_Z \sim 0.38\%$ [K. Fujii et al., arXiv:1710.07621 [hep-ex]]

  Direct searches by LHC Run-II :

  [A. Ilnicka, T. Robens, and T. Stefaniak, Mod. Phys. Lett. A33 no. 10n11, (2018) 1830007]

- We may be able to test the model by the synergy between measurements of the Higgs boson couplings and the spectrum of GW.

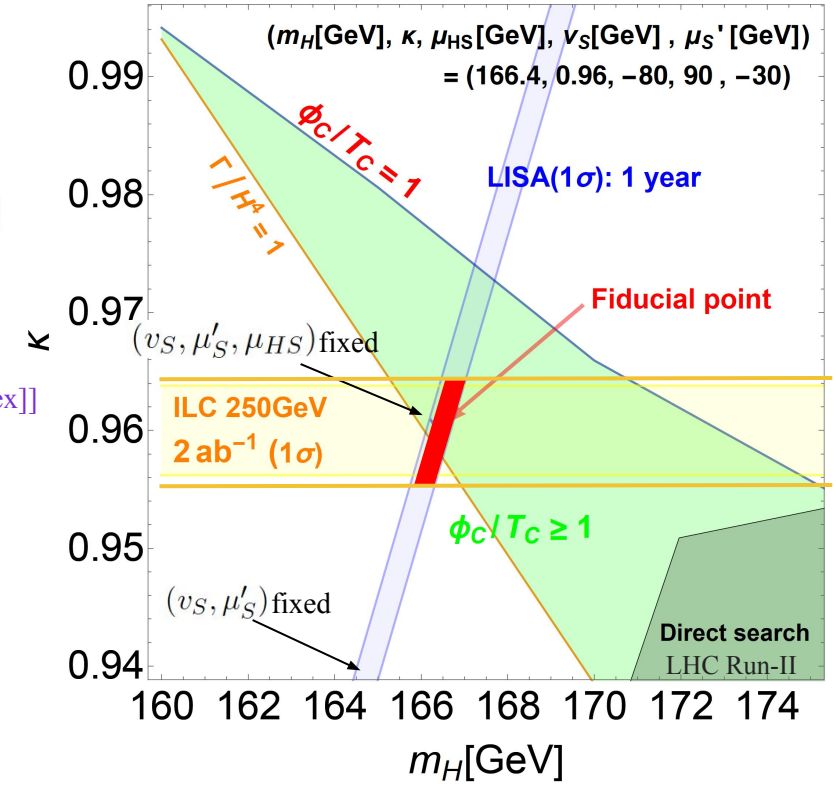

[K. H, R. Jinno, M. Kakizaki, S. Kanemura, T. Takahashi and M. Takimoto, Phys. Rev. D 99, no. 7, 075011 (2019)]

Testability of real Higgs singlet model

- $\Delta\lambda_{hhh}/\lambda_{hhh}^{SM}$ and detectable GWs are described in scaling factors (κ_F and κ_V) and m_H.

$$\frac{\Delta\lambda_{hhh}}{\lambda_{hhh}^{SM}} = \frac{\lambda_{hhh}-\lambda_{hhh}^{SM}}{\lambda_{hhh}^{SM}}, \quad \kappa_X \equiv \frac{g_{hXX}}{g_{hXX}^{\rm SM}}, \quad \kappa = \kappa_V = \kappa_F = \cos\theta$$

- Fiducial point (m_H, κ) = (166.4 GeV, 0.96)

  ILC : $\Delta\kappa_Z \sim 0.38\%$ [K. Fujii et al., arXiv:1710.07621 [hep-ex]]

  Direct searches by HL-LHC :

  [M. Carena, Z. Liu and M. Riembau, Phys. Rev. D 97, 095032 (2018)]

- We can test the model by HL-LHC (direct search), ILC (indirect search) and LISA (spectrum of GW).

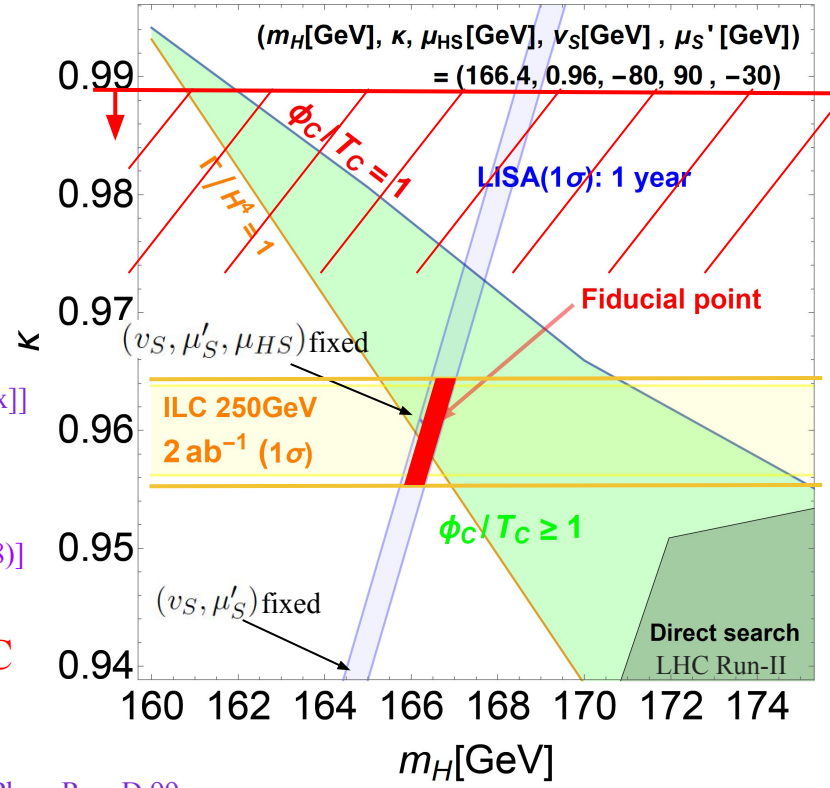

[K. H, R. Jinno, M. Kakizaki, S. Kanemura, T. Takahashi and M. Takimoto, Phys. Rev. D 99, no. 7, 075011 (2019)]

Summary

- The extended Higgs model can explain the phenomena beyond the Standard model, such as baryon asymmetry of the university.
- We have quantitatively discussed the testability of the model with strongly first-order electroweak phase transition by the collider and gravitational wave observation experiments.
- We can complementarily test the models by the measurements of the various Higgs boson couplings and direct search of new boson at the collider experiments and the spectrum of gravitational wave at the future space-based interferometers.

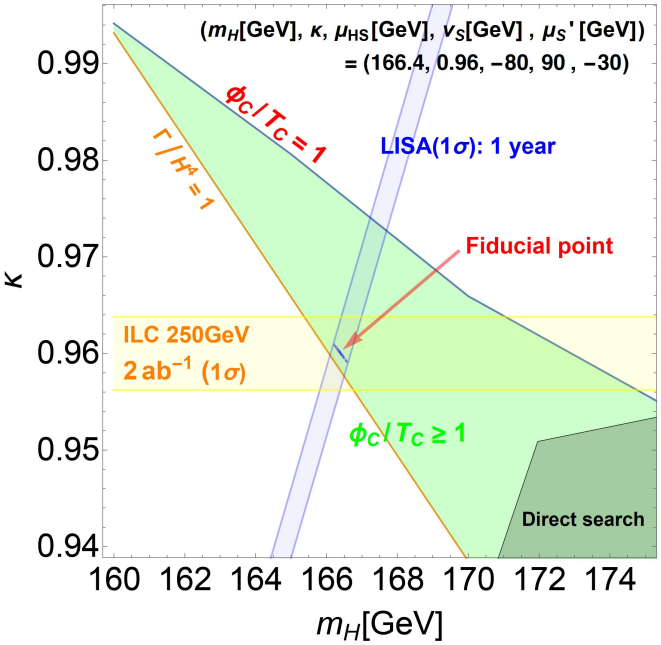

EWPT of the model with one singlet scalar field

- EWPT occurs in the space of two order parameters for doublet and singlet scalar.

It is the EWPT for one order parameter.

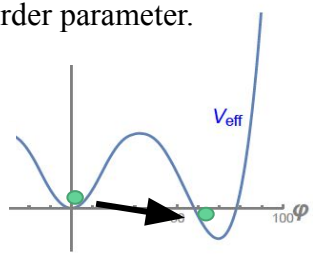

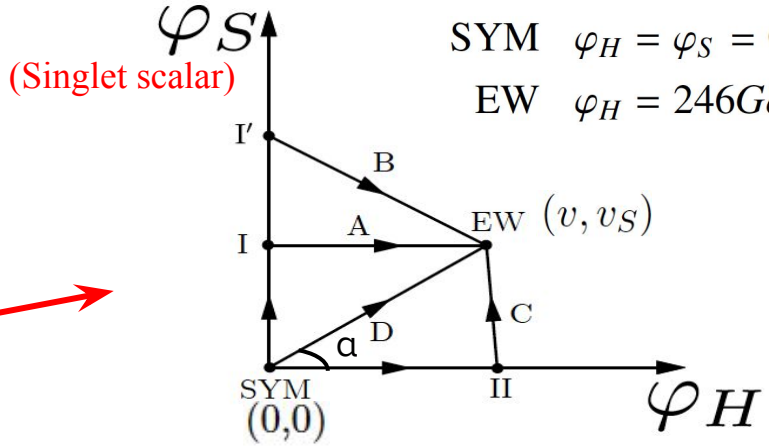

SYM $\varphi_H = \varphi_S = 0$ (False vacuum)

EW $\varphi_H = 246GeV,\ \varphi_S \neq 0$ (True vacuum)

- ϕ_c / T_c of the model with one singlet scalar field for Path A and B.

[S. Profumo, M. J. Ramsey-Musolf and G. Shaughnessy, JHEP 0708, 010 (2007)]

$$\phi_C/T_C \ni -\frac{2}{\lambda(T_C)}\left(\mu_{\Phi S}\cos^2\alpha + \frac{\mu'_S}{3}\sin^2\alpha\right)\sin\alpha/T_C$$

These are tree-level effects.

Backup

Fisher matrix analysis

Fisher matrix analysis

- Likelihood function

$$\delta\chi^2(\{p\},\{\hat{p}\}) := 2T_{\rm obs}\sum_{(I,I')}\int_0^\infty df\ \frac{\Gamma^2_{II'}(f)\left[S_h(f,\{p\})-S_h(f,\{\hat{p}\})\right]^2}{\sigma^2_{II'}(f)}. \qquad S_h(f)=\frac{3H_0^2}{2\pi^2}\frac{1}{f^3}\Omega_{\rm GW}(f)$$

Noise for detection of GW: $\sigma^2_{II'}(f)=[S_I(f)+\Gamma_{II}(f)S_h(f,\{\hat{p}\})]\,[S_{I'}(f)+\Gamma_{I'I'}(f)S_h(f,\{\hat{p}\})]+\Gamma^2_{II'}(f)S^2_h(f,\{\hat{p}\})$

$S_h(f,\{p\})$: GW spectrum for parameter set {p}, $\Gamma_{II'}$ is the overlap reduction function.

$S_{\rm eff}$: Effective sensitivity of interferometers,

$\{\hat{p}\}$: Fiducial parameter set, $T_{\rm obs}$: Observation period

Taylor expansion $\delta\chi^2(\{p\},\{\hat{p}\})\simeq\mathcal{F}_{ab}(p_a-\hat{p}_a)(p_b-\hat{p}_b)$ $\qquad \mathcal{F}_{ab}=2T_{\rm obs}\sum_{(I,I')}\int_0^\infty df\ \frac{\Gamma^2_{II'}(f)\partial_{p_a}S_h(f,\{\hat{p}\})\partial_{p_b}S_h(f,\{\hat{p}\})}{\sigma^2_{II'}(f)}$

[N. Seto, Phys. Rev. D 73, 063001 (2006)]

$$S_{\rm eff}(f)=\left[\sum_{(I,I')}\frac{\Gamma^2_{II'}(f)}{\sigma^{({\rm null})2}_{II'}(f)}\right]^{-1/2}$$

[E. Thrane and J. D. Romano, Phys. Rev. D 88, no. 12, 124032 (2013)]

Fisher matrix analysis

- Likelihood function

$$\delta\chi^2(\{p\},\{\hat{p}\}) = 2T_{\rm obs}\int_0^\infty df\,\frac{[S_h(f,\{p\})-S_h(f,\{\hat{p}\})]^2}{[S_{\rm eff}(f)+S_h(f,\{\hat{p}\})]^2}$$

Taylor expansion

$$\delta\chi^2(\{p\},\{\hat{p}\}) \simeq \mathcal{F}_{ab}(p_a-\hat{p}_a)(p_b-\hat{p}_b)$$

$$\mathcal{F}_{ab} = 2T_{\rm obs}\int_0^\infty df\,\frac{\partial_{p_a}S_h(f,\{\hat{p}\})\partial_{p_b}S_h(f,\{\hat{p}\})}{[S_{\rm eff}(f)+S_h(f,\{\hat{p}\})]^2}$$

$S_h(f,\{p\})$: GW spectrum for parameter set $\{p\}$,
$S_{\rm eff}$: Effective sensitivity of interferometers,
$\{\hat{p}\}$: Fiducial parameter set, $T_{\rm obs}$: Observation period

The inverse matrix of F_{ab} is the covariance matrix.

(We assume that we can apply the expression to one detector (LISA).)

- Sample point

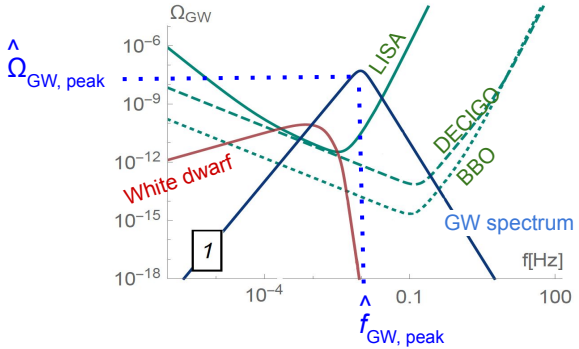

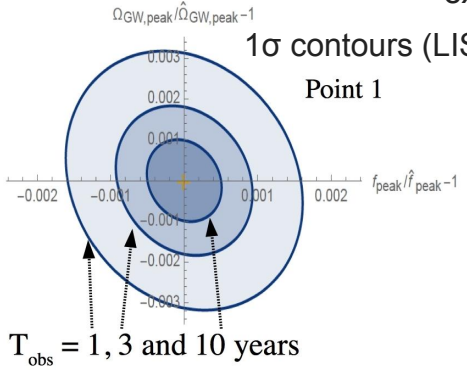

LISA, White dwarf : [A. Klein et al., Phys. Rev. D93 no. 2, (2016) 024003]

DECIGO, BBO : [K. Yagi and N. Seto, Phys. Rev. D83 (2011) 044011]

- The expected constraints on the GW spectrum propagate to the parameters in the model.

Fisher matrix analysis

❖ Effective sensitivity

- LISA

$$S_{\rm eff}(f) = \frac{20}{3}\frac{4S_{\rm acc}(f) + S_{\rm sn}(f) + S_{\rm omn}(f)}{L^2}\left[1 + \left(\frac{f}{0.41c/2L}\right)^2\right],$$

with $L = 5 \times 10^9$ m and

$$S_{\rm acc}(f) = 9 \times 10^{-30}\frac{1}{(2\pi f/1{\rm Hz})^4}\left(1 + \frac{10^{-4}}{f/1{\rm Hz}}\right)\ {\rm m^2 Hz^{-1}},$$
$$S_{\rm sn}(f) = 2.96 \times 10^{-23}\ {\rm m^2 Hz^{-1}},$$
$$S_{\rm omn}(f) = 2.65 \times 10^{-23}\ {\rm m^2 Hz^{-1}}.$$

[A. Klein et al., Phys. Rev. D93 no. 2, (2016) 024003]

- DECIGO

$$S_{\rm eff}(f) = \left[7.05 \times 10^{-48}\left[1 + (f/f_p)^2\right] + 4.8 \times 10^{-51}\frac{(f/1{\rm Hz})^{-4}}{1 + (f/f_p)^2} + 5.33 \times 10^{-52}(f/1{\rm Hz})^{-4}\right]\ {\rm Hz^{-1}},$$

with $f_p = 7.36$ Hz.

- BBO

$$S_{\rm eff}(f) = \left[2.00 \times 10^{-49}(f/1{\rm Hz})^2 + 4.58 \times 10^{-49} + 1.26 \times 10^{-52}(f/1{\rm Hz})^{-4}\right]\ {\rm Hz^{-1}}.$$

[K. Yagi and N. Seto, Phys. Rev. D83 (2011) 044011]

Fisher matrix analysis

- Noise for the white dwarf [A. Klein et al., Phys. Rev. D93 no. 2, (2016) 024003]

$$S'_{\rm WD}(f) = \begin{cases} (20/3)(f/1\ {\rm Hz})^{-2.3} \times 10^{-44.62}\ {\rm Hz}^{-1} & \equiv S^{(1)}_{\rm WD}(f) \quad (10^{-5}\ {\rm Hz} < f < 10^{-3}\ {\rm Hz}), \\ (20/3)(f/1\ {\rm Hz})^{-4.4} \times 10^{-50.92}\ {\rm Hz}^{-1} & \equiv S^{(2)}_{\rm WD}(f) \quad (10^{-3}\ {\rm Hz} < f < 10^{-2.7}\ {\rm Hz}), \\ (20/3)(f/1\ {\rm Hz})^{-8.8} \times 10^{-62.8}\ {\rm Hz}^{-1} & \equiv S^{(3)}_{\rm WD}(f) \quad (10^{-2.7}\ {\rm Hz} < f < 10^{-2.4}\ {\rm Hz}), \\ (20/3)(f/1\ {\rm Hz})^{-20.0} \times 10^{-89.68}\ {\rm Hz}^{-1} & \equiv S^{(4)}_{\rm WD}(f) \quad (10^{-2.4}\ {\rm Hz} < f < 10^{-2}\ {\rm Hz}). \end{cases}$$

$$S_{\rm WD}(f) = \frac{1}{1/S^{(1)}_{\rm WD}(f) + 1/S^{(2)}_{\rm WD}(f) + 1/S^{(3)}_{\rm WD}(f) + 1/S^{(4)}_{\rm WD}(f)}$$

$$S_{\rm WD} \simeq \max(S^{(1)}_{\rm WD}, S^{(2)}_{\rm WD}, S^{(3)}_{\rm WD}, S^{(4)}_{\rm WD})$$

Fisher matrix analysis

- The expected uncertainties for LISA at Fiducial point (m_H, κ) = (166.4 GeV, 0.96) (Blue ellipeses and bands)

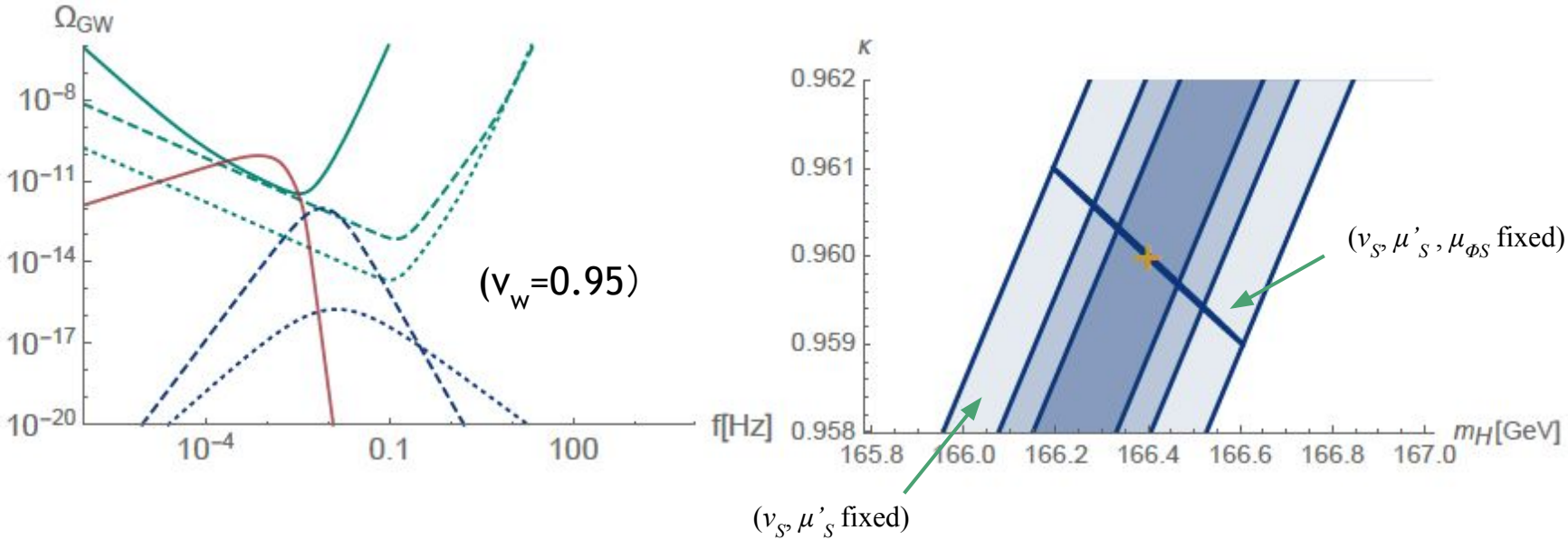

Fisher matrix analysis

- Noise for binary neutron stars and binary black holes (Stochastic GW)

[Virgo, LIGO Scientic Collaboration, B. P. Abbott et al., arXiv:1710.05837 [gr-qc]]

$$S_{\mathrm{NSBH}}(f) = \frac{3H_0^2}{2\pi^2}\frac{1}{f^3} \times 1.8 \times 10^{-8} \left(\frac{f}{25\ \mathrm{Hz}}\right)^{\frac{2}{3}} \qquad 10\ \mathrm{Hz} < f < 10^3\ \mathrm{Hz}$$

→ This noise does not affect our analysis, because frequency of the noise is small.

(We tried to extrapolate the noise to 1 Hz, but our result doesn't change.)

Others

Gravitational waves interferometers

❖ If electroweak phase transition (EWPT) is 1st order, gravitational waves (GWs) occur from EWPT.

★ Ground-based GWs interferometers (LIGO, KAGRA, Advanced Virgo, …)

→ These experiments can detect GWs from astronomical origin.

LIGO detected GWs directly. [PRL.116, no. 6,061102(2016), PRL.116, no. 24, 241103(2016), PRL. 118, no. 22, 221101 (2017), PRL. 119, no. 14, 141101 (2017), PRL 119, no. 16, 161101 (2017)]

★ Future space-based GWs interferometers (LISA, DECIGO, ...)

LISA is scheduled to launch into space in 2034.

→ These experiments can detect GWs from the early universe such as electroweak 1stOPT, and so on.

The measurements of the deviations

- The measurement of κ [Snowmass Higgs Working Group Report (1310.8361)] [K. Fujii et al., arXiv:1710.07621 [hep-ex]]

Facility	LHC	HL-LHC	ILC500	ILC500-up
$\sqrt{s}$ (GeV)	14,000	14,000	250/500	250/500
$\int \mathcal{L}dt$ (fb^{-1})	300/expt	3000/expt	250+500	1150+1600
κ_γ	$5-7\%$	$2-5\%$	8.3%	4.4%
κ_g	$6-8\%$	$3-5\%$	2.0%	1.1%
κ_W	$4-6\%$	$2-5\%$	0.39%	0.21%
κ_Z	$4-6\%$	$2-4\%$	0.49%	0.24%
κ_ℓ	$6-8\%$	$2-5\%$	1.9%	0.98%
$\kappa_d = \kappa_b$	$10-13\%$	$4-7\%$	0.93%	0.60%
$\kappa_u = \kappa_t$	$14-15\%$	$7-10\%$	2.5%	1.3%

ILC 250GeV 2000fb^{-1}	
hbb	1.8%
hcc	2.4%
hgg	2.2%
hWW	1.8%
$h\tau\tau$	1.9%
hZZ	0.38%
$h\gamma\gamma$	1.1%
$h\mu\mu$	5.6%

- The measurement of λ_{hhh} [S.Dawson et al.,arXiv:1310.8361] [K.Fujii et al., arXiv:1506.05992]

	HL-LHC 14 TeV 3000fb^{-1}	ILC 500GeV 4000fb^{-1}	ILC 1TeV 2000fb^{-1}(5000fb^{-1})
λ_{hhh}	50%	27%	16% (10%)

The measurements of the deviations

Parameter	ATLAS+CMS
	Measured
κ_Z	1.00 $[0.92, 1.00]$
κ_W	0.90 $[0.81, 0.99]$
κ_t	$1.43^{+0.23}_{-0.22}$
$\lvert\kappa_\tau\rvert$	$0.87^{+0.12}_{-0.11}$
$\lvert\kappa_b\rvert$	$0.57^{+0.16}_{-0.16}$
$\lvert\kappa_g\rvert$	$0.81^{+0.13}_{-0.10}$
$\lvert\kappa_\gamma\rvert$	$0.90^{+0.10}_{-0.09}$

["ATLAS and CMS Collaborations" JHEP 1608, 045 (2016)]

The measurements of the deviations

Facility	LHC	HL-LHC	ILC500	ILC 250
$\sqrt{s}$ (GeV)	14,000	14,000	250/500	250
$\int \mathcal{L}dt$ (fb^{-1})	300/expt	3000/expt	250+500	2000
κ_γ	$5-7\%$	$2-5\%$	8.3%	1.1%
κ_g	$6-8\%$	$3-5\%$	2.0%	2.2%
κ_W	$4-6\%$	$2-5\%$	0.39%	1.8 %
κ_Z	$4-6\%$	$2-4\%$	0.49%	0.38%
κ_τ	$6-8\%$	$2-5\%$	1.9%	1.9%
κ_b	$10-13\%$	$4-7\%$	0.93%	1.8 %
κ_t	$14-15\%$	$7-10\%$	2.5%	-

Snowmass Higgs Working Group Report (1310.8361)

The measurements of the deviations

	ILC250		+ILC500	
	κ fit	EFT fit	κ fit	EFT fit
$g(hbb)$	1.8	1.1	0.60	0.58
$g(hcc)$	2.4	1.9	1.2	1.2
$g(hgg)$	2.2	1.7	0.97	0.95
$g(hWW)$	1.8	0.67	0.40	0.34
$g(h\tau\tau)$	1.9	1.2	0.80	0.74
$g(hZZ)$	0.38	0.68	0.30	0.35
$g(h\gamma\gamma)$	1.1	1.2	1.0	1.0
$g(h\mu\mu)$	5.6	5.6	5.1	5.1
$g(h\gamma Z)$	16	6.6	16	2.6
$g(hbb)/g(hWW)$	0.88	0.86	0.47	0.46
$g(h\tau\tau)/g(hWW)$	1.0	1.0	0.65	0.65
$g(hWW)/g(hZZ)$	1.7	0.07	0.26	0.05
Γ_h	3.9	2.5	1.7	1.6
$BR(h \to inv)$	0.32	0.32	0.29	0.29
$BR(h \to other)$	1.6	1.6	1.3	1.2

For example,

$$\frac{\Gamma(h \to ZZ^*)}{SM} = \kappa_Z^2 , \qquad \frac{\sigma(e^+e^- \to Zh)}{SM} = \kappa_Z^2$$

where SM denotes the SM prediction.

K. Fujii et al., arXiv:1710.07621 [hep-ex]

(New physics effects)

$$\delta\mathcal{L} = \frac{m_Z^2}{v}(1+\eta_Z)hZ_\mu Z^\mu + \zeta_Z \frac{1}{v} hZ_{\mu\nu}Z^{\mu\nu}$$

In the κ formalism, the couplings ζ_Z, ζ_W are assumed to be zero.

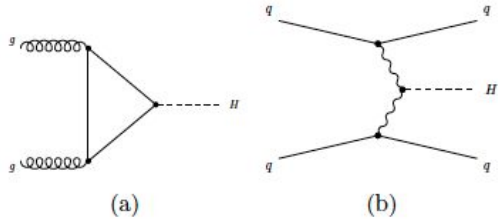

Figure 1. Examples of leading-order Feynman diagrams for Higgs boson production via the (a) ggF and (b) VBF production processes.

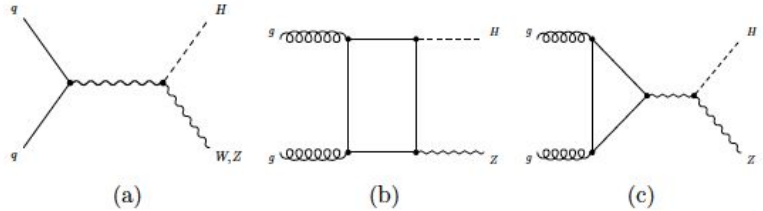

Figure 2. Examples of leading-order Feynman diagrams for Higgs boson production via the (a) $qq \to VH$ and (b, c) $gg \to ZH$ production processes.

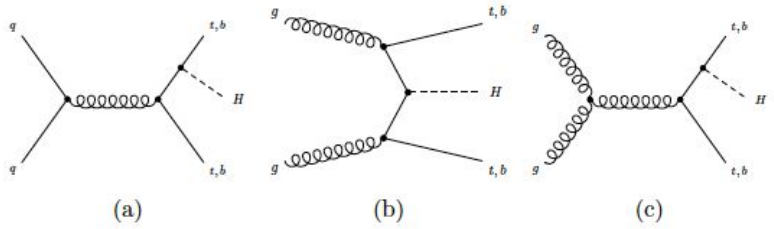

Figure 3. Examples of leading-order Feynman diagrams for Higgs boson production via the $qq/gg \to ttH$ and $qq/gg \to bbH$ processes.

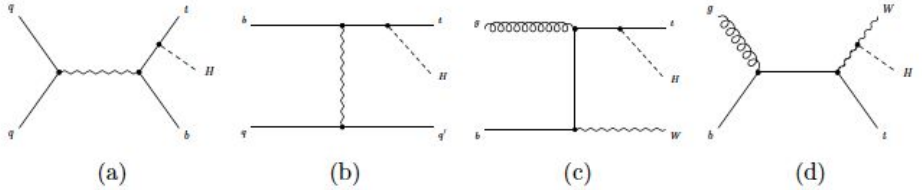

Figure 4. Examples of leading-order Feynman diagrams for Higgs boson production in association with a single top quark via the (a, b) tHq and (c, d) tHW production processes.

- gluon fusion production $gg \to H$ (figure 1a);
- vector boson fusion production $qq \to qqH$ (figure 1b);
- associated production with a W boson, $qq \to WH$ (figure 2a), or with a Z boson, $pp \to ZH$, including a small ($\sim$ 8%) but less precisely known contribution from $gg \to ZH$ ($ggZH$) (figures 2a, 2b, and 2c);
- associated production with a pair of top quarks, $qq, gg \to ttH$ (figure 3).

Other less important production processes in the SM, which are not the target of a direct search but are included in the combination, are $qq, gg \to bbH$ (bbH), also shown in figure 3, and production in association with a single top quark (tH), shown in figure 4. The latter process proceeds through either $qq/qb \to tHb/tHq'$ (tHq) (figures 4a and 4b) or $gb \to tHW$ (tHW) (figures 4c and 4d) production.

[G. Aad et al. [ATLAS and CMS Collaborations], JHEP 1608, 045 (2016)]

Figure 2.7
Production cross section for the $e^+e^- \to Zh$ process as a function of the center of mass energy for $m_h = 125\,\text{GeV}$, plotted together with those for the WW and ZZ fusion processes: $e^+e^- \to \nu\bar{\nu}H$ and $e^+e^- \to e^+e^-H$.

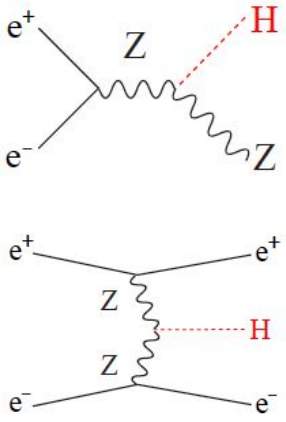

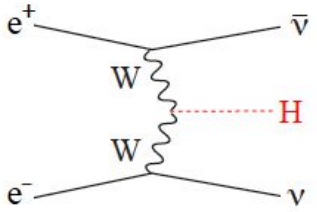

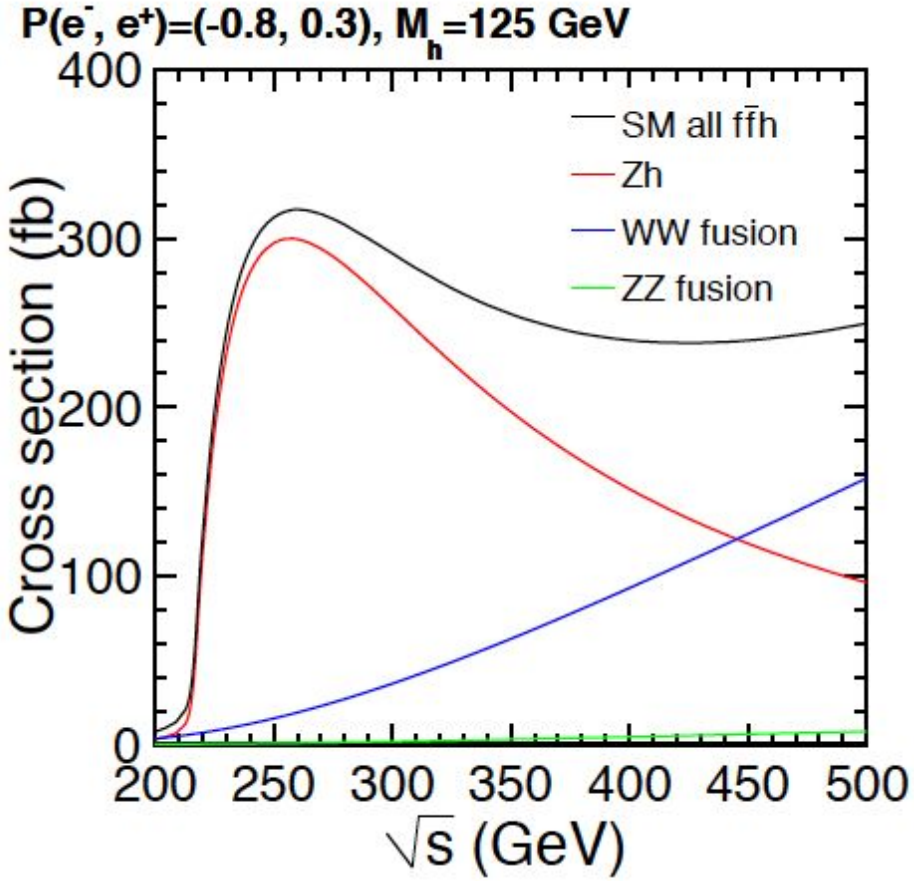

H. Baer et al., arXiv:1306.6352 [hep-ph].

High temperature expansion

The loop effect of bosons and fermions

$$V_{eff}(\varphi, T) = D(T^2 - T_0^2)\varphi^2 - (ET - e)\varphi^3 + \frac{\lambda(T)}{4}\varphi^4$$

The loop effect of bosons

The effect of mixing Higgs fields

$$\frac{\varphi_c}{T_c} = \frac{2E}{\lambda}\left(1 - \frac{e\lambda}{ET}\right)$$

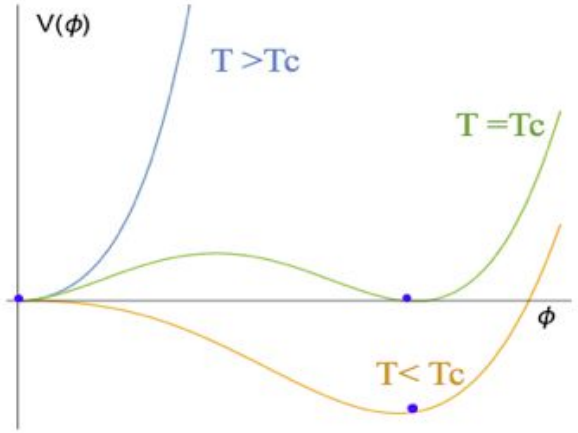

Landau pole

- Potential

$$V_0 = -\mu_\Phi^2|\Phi|^2 + \lambda_\Phi|\Phi|^4 + \mu_{\Phi S}|\Phi|^2 S + \frac{\lambda_{\Phi S}}{2}|\Phi|^2 S^2 + \mu_S^3 S + \frac{m_S^2}{2}S^2 + \frac{\mu'_S}{3}S^3 + \frac{\lambda_S}{4}S^4$$

- Benchmark point

v_Φ [GeV]	v_S [GeV]	m_h [GeV]	$\mu_{\Phi S}$ [GeV]	μ'_S [GeV]	μ_S [GeV]	m_H [GeV]	θ [degrees]
246.2	90	125.5	−80	−30	0	170	-20

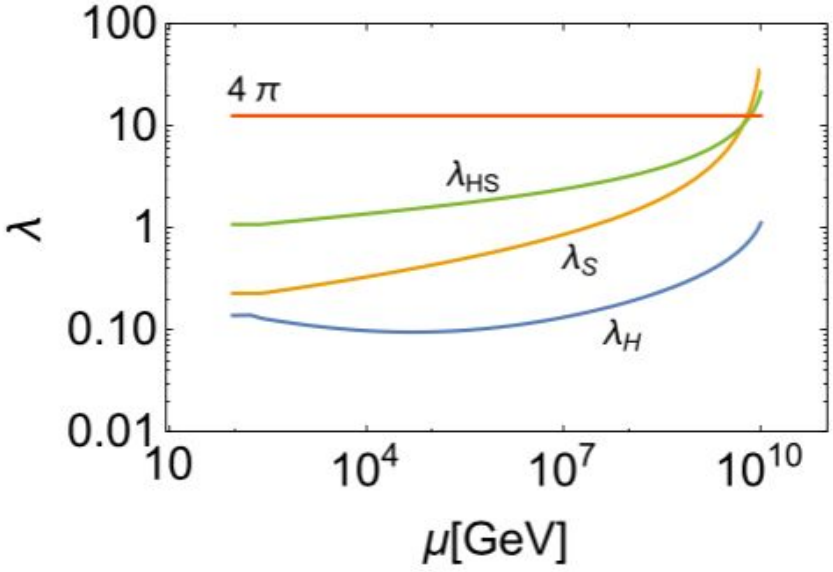

Running of scalar coupling

$$\lambda_{hhh}^{\text{HSM}} = c_\theta^3 \left\langle \frac{\partial^3 V_{\text{eff},T=0}}{\partial \varphi_\Phi^3} \right\rangle + c_\theta^2 s_\theta \left\langle \frac{\partial^3 V_{\text{eff},T=0}}{\partial \varphi_\Phi^2 \partial \varphi_S} \right\rangle + c_\theta s_\theta^2 \left\langle \frac{\partial^3 V_{\text{eff},T=0}}{\partial \varphi_\Phi \partial \varphi_S^2} \right\rangle + s_\theta^3 \left\langle \frac{\partial^3 V_{\text{eff},T=0}}{\partial \varphi_S^3} \right\rangle$$

$$V_0 = -\mu_\Phi^2 |\Phi|^2 + \lambda_\Phi |\Phi|^4 + \mu_{\Phi S} |\Phi|^2 S + \frac{\lambda_{\Phi S}}{2} |\Phi|^2 S^2 + \mu_S^3 S + \frac{m_S^2}{2} S^2 + \frac{\mu'_S}{3} S^3 + \frac{\lambda_S}{4} S^4$$

$$+ \mu_S^3 S + \frac{m_S^2}{2} S^2 + \frac{\mu'_S}{3} S^3 + \frac{\lambda_S}{4} S^4$$

v_Φ [GeV]	v_S [GeV]	m_h [GeV]	$\mu_{\Phi S}$ [GeV]	μ'_S [GeV]	μ_S [GeV]	m_H [GeV]	θ [degrees]
246.2	90	125.5	-80	-30	0	[160, 240]	$[-45, 0]$

Constraints

- Perturbative unitarity

$$m_h^2 \cos^2\theta + m_H^2 \sin^2\theta \leq \frac{4\pi\sqrt{2}}{3G_F} \approx (700\text{GeV})^2$$

- Vacuum stability

$$\lambda_\Phi(\mu) > 0, \qquad \lambda_S(\mu) > 0, \qquad 4\lambda_\Phi(\mu)\lambda_S(\mu) > \lambda_{\Phi S}^2(\mu)$$

- Oblique parameters

$$\cos\theta \gtrsim 0.92 \quad \text{when } m_H \gtrsim 400\text{GeV } (m_h \approx 125\text{GeV})$$

[S. Baek, P. Ko, W. I. Park and E. Senaha, JHEP 1211, 116 (2012)]

Direct search

[T. Robens and T. Stefaniak, Eur. Phys. J. C 76, no. 5, 268 (2016)]

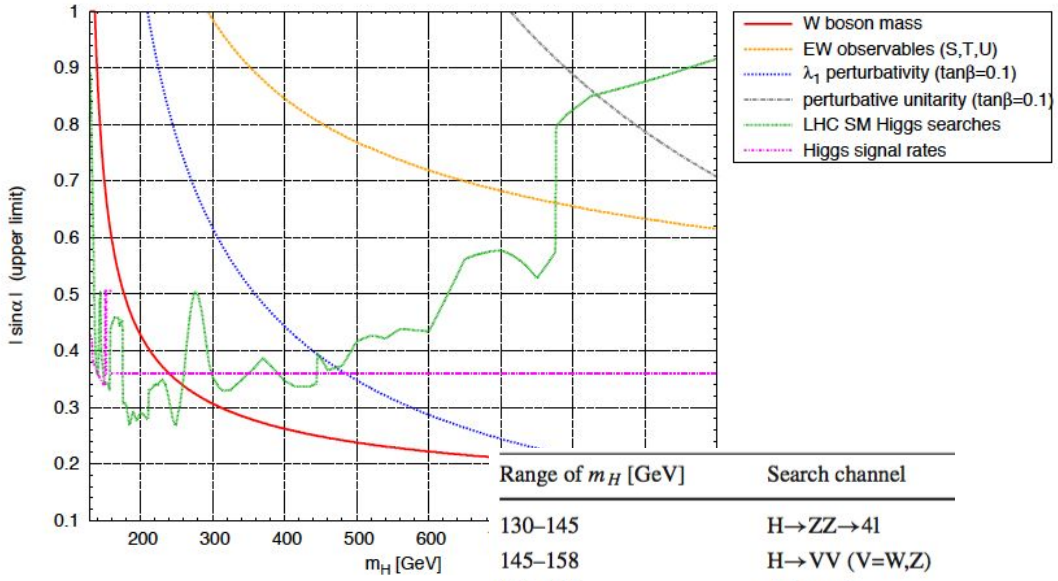

Range of m_H [GeV]	Search channel
130–145	H→ZZ→4l
145–158	H→VV (V=W,Z)
158–163	SM comb.
163–170	H→WW
170–176	SM comb.
176–211	H→VV (V=W,Z)
211–225	H→ZZ→4l
225–445	H→VV (V=W,Z)
445–776	H→ZZ
776–1000	H→VV (V=W,Z)

Direct search

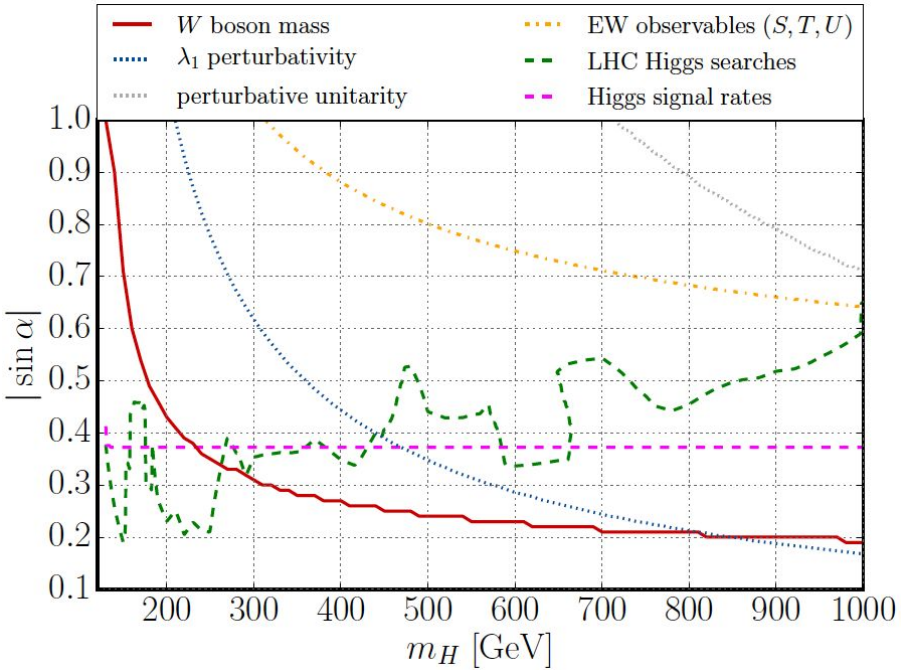

Fig. 1. Constraints on the mixing angle, $|\sin\alpha|$, as a function of the additional Higgs boson mass, m_H, in the real singlet extension of the SM (for fixed $\tan\beta = 0.1$): Theoretical constraints from perturbativity of the couplings (*dotted blue*), perturbative unitarity (*dotted gray*), and experimental constraints from the W-boson mass (*solid red*), electroweak precision observables (*dot-dashed orange*), LHC Higgs searches for additional Higgs bosons (*dashed green*) and LHC measurements of the Higgs signal rates (*dashed magenta*).

[A. IlnickaT. Robens and T. Stefaniak, arXiv:1803.03594]

$\tan\beta \equiv v/x$ x : VEV for singlet scalar field

The constraint on singlet scalar field HL-LHC

$v_s = v \tan\beta$

[M. Carena, Z. Liu and M. Riembau, Phys. Rev. D 97, 095032 (2018)]

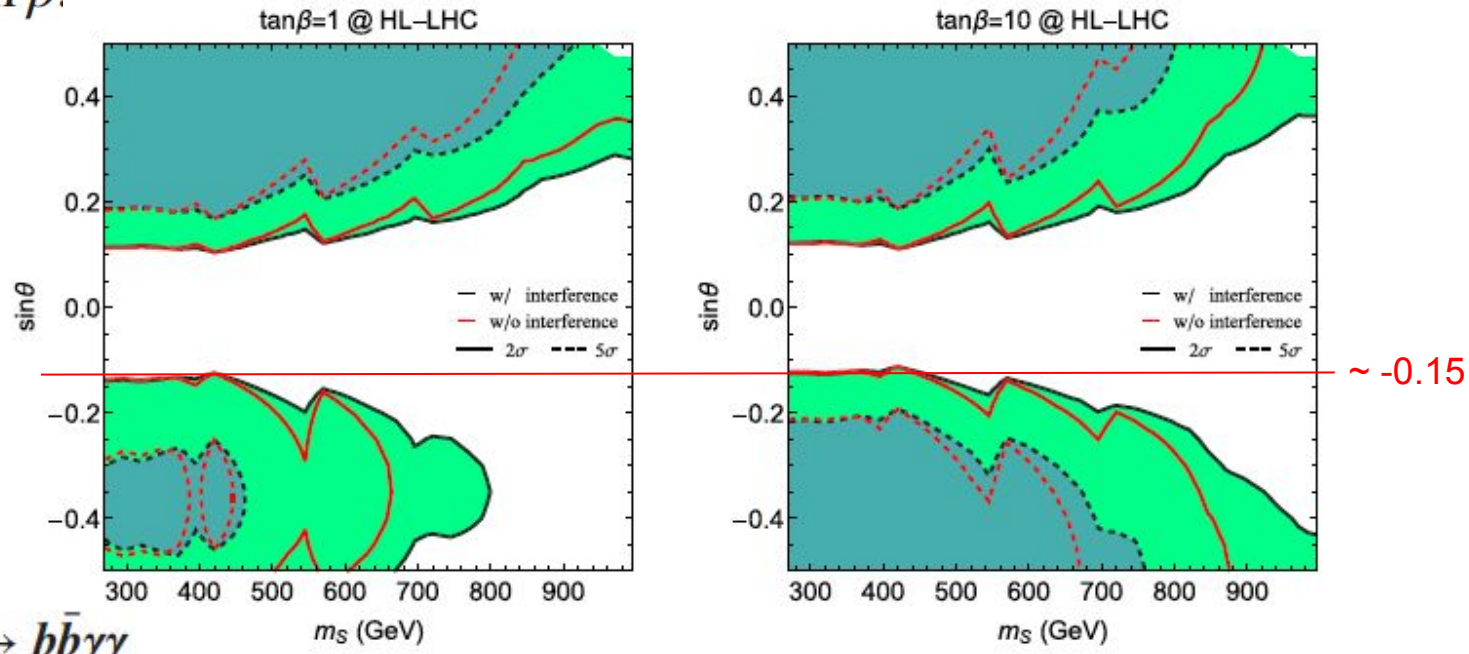

$pp \to HH \to b\bar{b}\gamma\gamma$

FIG. 9. Projected exclusion and discovery limits at HL-LHC in the m_S- $\sin\theta$ plane with the line-shape analysis detailed in the text for $\tan\beta = 1$ (left panel) and $\tan\beta = 10$ (right panel). The shaded regions bounded by dashed/solid curves are within the discovery/ exclusion reach of the HL-LHC. The black and red lines represent the projection with and without the inclusion of the interference effects between the singlet resonance diagram and the SM Higgs pair diagram, respectively.

The constraint on singlet scalar field HL-LHC

$$v_s = v \tan\beta.$$

[M. Carena, Z. Liu and M. Riembau, Phys. Rev. D 97, 095032 (2018)]

TABLE II. Summary of expected number of events for the SM Higgs pair production and the SM backgrounds for the $b\bar{b}\gamma\gamma$ di-Higgs search after selection cuts, obtained from Ref. [61] for the HL-LHC and further extrapolated for the HE-LHC.

# of events expected bins (GeV)	HL-LHC 13 TeV @ 3 ab^{-1}		HE-LHC 27 TeV @ 10 ab^{-1}	
	SM HH	SM BKG	SM HH	SM BKG
250–400	2.1	12.0	33.2	186.4
400–550	6.3	15.9	110.9	278.8
550–700	2.9	5.2	58.4	105.6
700–850	1.0	2.0	23.4	46.7
850–1000	0.3	1.4	8.9	38.8
1000–1200	0.2	0.7	4.7	20.4
1200–1400	···	···	1.9	8.0
1400–1600	···	···	0.8	3.5
1600–1800	···	···	0.4	1.7
1800–2000	···	···	0.2	0.9

$$pp \to HH \to b\bar{b}\gamma\gamma$$

To extrapolate the signal expected from our singlet extension of the SM, we assume the same acceptance as the SM Higgs pair.

We assume that the observed number of events in this channel follows the SM expectation values.

GW spectrum from 1stOPT

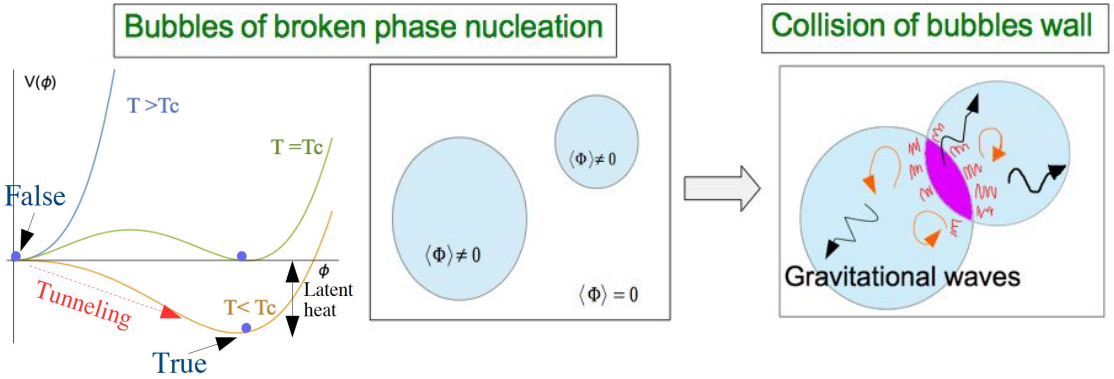

$$S_3 \equiv \int d^3r \left[\frac{1}{2}(\vec{\nabla}\varphi)^2 + V_{\text{eff}}(\varphi, T)\right]$$

- The bubble nucleation rate per unit volume per unit time: $\Gamma(T) \simeq T^4 e^{-\frac{S_3(T)}{T}}$
- Transition temperature T_t : $\Gamma/H^4|_{T=T_t} = 1$

  (The temperature at the end of phase transition)

(S_3 : the three dimensional Euclidean action
H : the Hubble parameter)

- The GW spectrum is characterized by α and β : $\Omega_{\text{GW}} \propto \left(\frac{H}{\beta}\right)^n \left(\frac{\kappa\alpha}{1+\alpha}\right)^m$

"Bubble collision(Envelope approximation) n=2, m=2" [M. Kamionkowski, A. Kosowsky and M. S. Turner, Phys. Rev. D 49, 2837 (1994)]

α ≈ Normalized latent heat released by PT, β ≈ 1/(The duration of PT)

$$\alpha = \frac{\epsilon(T_t)}{\rho_{rad}(T_t)}, \quad \beta \simeq \frac{1}{\Gamma}\frac{d\Gamma}{dT}$$

Latent heat : $\epsilon(T) = -V_{\text{eff}}(\varphi_B(T), T) + T\frac{\partial V_{\text{eff}}(\varphi_B(T), T)}{\partial T}$

Radiative energy dencity : ρ_{rad}

Phase transition

- The bubble nucleation rate per unit volume per unit time:

$$\Gamma(T) \simeq T^4 e^{-\frac{S_3(T)}{T}} \qquad \left(S_3 = \int d^3r \left[\frac{1}{2} (\vec{\nabla}\varphi_b)^2 + V_{\text{eff}}(\varphi_b, T) \right] \right)$$

- The bounce solution φ_b is obtained by equation of motion.

$$\frac{d^2\varphi_b}{dr^2} + \frac{2}{r}\frac{d\varphi_b}{dr} - \frac{\partial V_{\text{eff}}}{\partial \varphi_b} = 0$$

Boundary condition $\left. \frac{d\varphi_b}{dr} \right|_{r=0} = 0, \quad \lim_{r\to\infty} \varphi_b = 0$

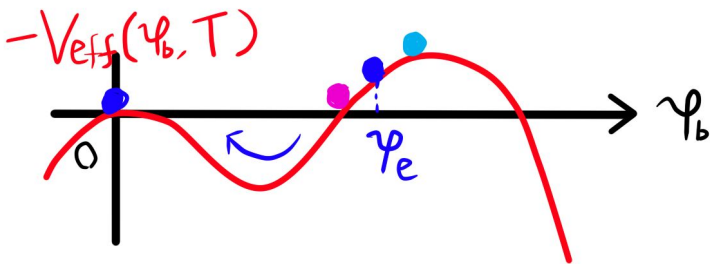

Phase transition

- The bounce solution φ_b is obtained by equation of motion.

$$\frac{d^2\varphi_b}{dr^2} + \frac{2}{r}\frac{d\varphi_b}{dr} - \frac{\partial V_{\text{eff}}}{\partial \varphi_b} = 0$$

(Boundary condition $\left.\frac{d\varphi_b}{dr}\right|_{r=0} = 0, \quad \lim_{r\to\infty} \varphi_b = 0$)

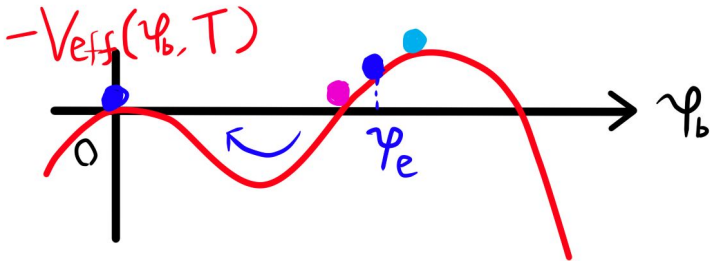

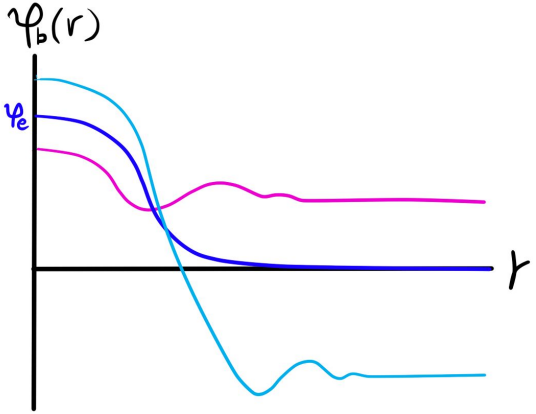

- We can obtain S_b by the bounce solution φ_b.

$$\rightarrow \quad \frac{S_3(T_t)}{T_t} = 4\ln(T_t/H_t) \simeq 140$$ (We can obtain T_t by the equation.)

The spectrum of the stochastic GWs

[C. Caprini, et al., J. Cosmol. Astropart. Phys. 1604 (04) (2016) 001.]

➢ Compression wave of plasma

$$\widetilde{\Omega}_{\rm sw}h^2 \simeq 2.65\times10^{-6}v_b\tilde{\beta}^{-1}\left(\frac{\kappa_v\alpha}{1+\alpha}\right)^2\left(\frac{100}{g_*^t}\right)^{1/3}$$ the peak of energy dencity

$$\tilde{f}_{\rm sw} \simeq 1.9\times10^{-5}\ {\rm Hz}\frac{1}{v_b}\tilde{\beta}\left(\frac{T_t}{100\ {\rm GeV}}\right)\left(\frac{g_*^t}{100}\right)^{1/6}$$ the peak frequency

$$\Omega_{\rm sw}(f)h^2 = \widetilde{\Omega}_{\rm sw}h^2\times(f/\tilde{f}_{\rm sw})^3\left(\frac{7}{4+3(f/\tilde{f}_{\rm sw})^2}\right)^{7/2}$$

In this talk, we use only the GW spectrum from compression wave pf plasma.

➢ Collision of wall

$$\widetilde{\Omega}_{\rm env}h^2 \simeq 1.67\times10^{-5}\times\left(\frac{0.11v_b^3}{0.42+v_b^2}\right)\tilde{\beta}^{-2}\left(\frac{\kappa_\varphi\alpha}{1+\alpha}\right)^2\left(\frac{100}{g_*^t}\right)^{1/3}$$

$$\tilde{f}_{\rm env} \simeq 1.65\times10^{-5}\ {\rm Hz}\times\left(\frac{0.62}{1.8-0.1v_b+v_b^2}\right)\tilde{\beta}\left(\frac{T_t}{100\ {\rm GeV}}\right)\left(\frac{g_*^t}{100}\right)^{1/6}$$

➢ Plasma turbulence

$$\widetilde{\Omega}_{\rm turb}h^2 \simeq 3.35\times10^{-4}v_b\tilde{\beta}^{-1}\left(\frac{\epsilon\kappa_v\alpha}{1+\alpha}\right)^{3/2}\left(\frac{100}{g_*^t}\right)^{1/3}$$

$$\tilde{f}_{\rm turb} \simeq 2.7\times10^{-5}\ {\rm Hz}\frac{1}{v_b}\tilde{\beta}\left(\frac{T_t}{100\ {\rm GeV}}\right)\left(\frac{g_*^t}{100}\right)^{1/6}$$

$\kappa_\varphi, \kappa_v, \epsilon$: efficiency factors $\quad$ v_b: wall velocity

[J.R.Espinosa,T.Konstandin, J.M.No and G. Servant,JCAP 1006,028 (2010)]

Efficiency factors

[J. R. Espinosa, T. Konstandin, J. M. No and G. Servant, JCAP 1006, 028 (2010)]

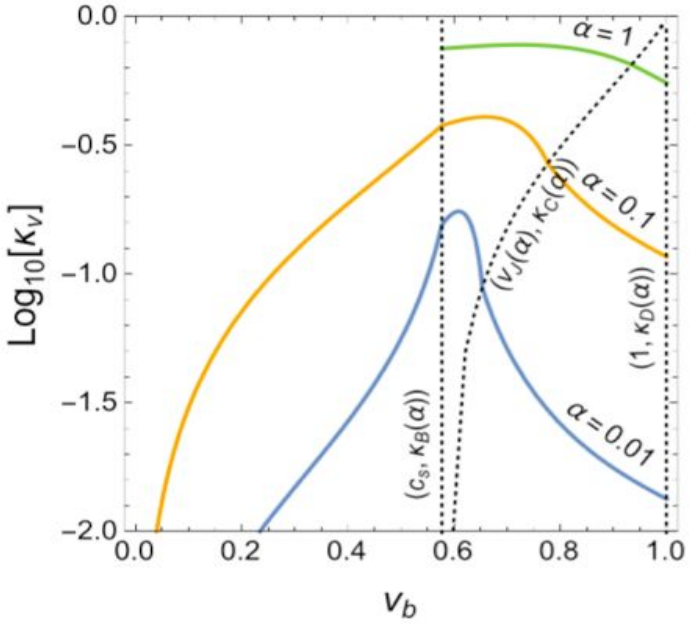

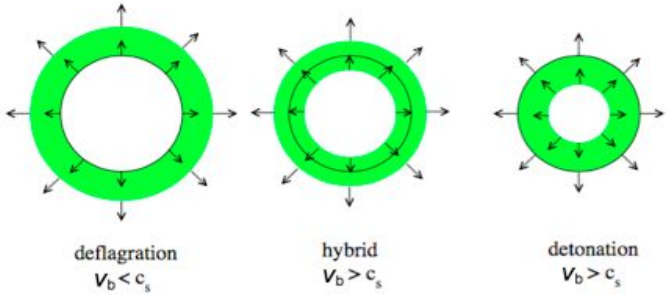

The black circle is bubble wall.
In green we show the region of non-zero fluid velocity.

ϵ: 5-10%. (In our numerical analysis, we set $\epsilon = 0.05$.)

[M.Hindmarsh et al.,Phys. Rev. D92, no. 12, 123009 (2015)]